https://doi.org/10.31925/farmacia.2026.3.8 **ORIGINAL ARTICLE**

SYNTHESIS, MOLECULAR DOCKING, AND PHARMACOLOGICAL EVALUATION OF NOVEL AMIDES OF 2-(3-(1-BENZYL-5-OXOPYRROLIDIN-3-YL)-5-THIOXO-4,5-DIHYDRO-1H-1,2,4-TRIAZOL-4-YL)ACETIC ACID AS POTENTIAL NOOTROPIC AGENTS

LINA PEREKHODA [1], RUSTAM SULEIMAN [1], ANTON SEMENETS [2], SERGII SHTRYGOL [3], MARHARYTA SULEIMAN [1]*, NATALIIA KOBZAR [1], VITALIY YAREMENKO [1], VICTORIYA GEORGIYANTS [1], SERGIY M. KOVALENKO [4]

[1]*Department of Pharmaceutical Chemistry, National University of Pharmacy, 61002, Kharkiv, Ukraine*
[2]*Bayer Limited Liability Company, 0407, Kyiv, Ukraine*
[3]*Department of Pharmacology and Clinical Pharmacy, National University of Pharmacy, 61002, Kharkiv, Ukraine*
[4]*Department of Organic Chemistry and Molecular Materials, V.N.Karazin Kharkiv National University, 61077, Kharkiv, Ukraine*

**corresponding author: sul.margo88@gmail.com*

Manuscript received: February 2025

Abstract

Pyrrolidone derivatives are promising substances for supporting and restoring cognitive functions in various etiological forms and disorders. The search for active molecules in this class of substances is becoming increasingly relevant, particularly in connection with the prevalence of post-COVID-19 cognitive deficits, neurodegenerative diseases, and traumatic brain injuries. In order to obtain new potential nootropics, a chemical modification of the synthetic framework we previously obtained, 1-benzyl-4-(5-sulfanylidene-4,5-dihydro-1H-1,2,4-triazol-3-yl)pyrrolidin-2-one, was carried out by introducing an acetate group and subsequent amidation with the corresponding amines. The structure and purity of the obtained amides were confirmed by elemental analysis, ^{1}H NMR spectroscopy, ^{13}C NMR spectroscopy, and LC/MS. The effectiveness of the performed chemical modification was confirmed by molecular docking to the nootropic biomolecules, the α-amino-3-hydroxy-5-methyl-4-isoxazolepropionic acid (AMPA) receptor and the muscarinic (M1) acetylcholine receptor, as well as by pharmacological studies of antiamnesic activity. In the passive avoidance test in mice, the most promising compound, 1-benzyl-4-{4-[2-oxo-2-(piperidin-1-yl)ethyl]-5-sulfanylidene-4,5-dihydro-1H-1,2,4-triazol-3-yl}pyrrolidine-2-one 9d, was found, which eliminated the amnesic effect of scopolamine: 100% of the animals that had reached the learning criterion, and the antiamnesic activity was 106.4%.

Rezumat

În cadrul acestui studiu, pentru obținerea unor noi compuși cu potențial nootrop, a fost realizată modificarea chimică a structurii sintetice obținute anterior, 1-benzil-4-(5-sulfaniliden-4,5-dihidro-1H-1,2,4-triazol-3-il)pirolidin-2-onă, prin introducerea unei grupări acetat, urmată de amidare cu aminele corespunzătoare. Structura și puritatea amidelor obținute au fost confirmate prin analiză elementală, spectroscopie RMN ^{1}H, spectroscopie RMN ^{13}C și cromatografie lichidă cuplată cu spectrometrie de masă (LC/MS). Eficiența modificării chimice realizate a fost susținută atât prin studii de andocare moleculară asupra unor biomolecule relevante pentru activitatea nootropă, receptorul α-amino-3-hidroxi-5-metil-4-izoxazolpropionic (AMPA) și receptorul muscarinic colinergic M1, cât și prin evaluarea farmacologică a activității antiamnezice. În testul de evitare pasivă efectuat la șoareci, cel mai promițător compus identificat a fost 1-benzil-4-{4-[2-oxo-2-(piperidin-1-il)etil]-5-sulfaniliden-4,5-dihidro-1H-1,2,4-triazol-3-il}pirolidin-2-onă (9d), care a contracarat efectul amnezic indus de scopolamină: 100% dintre animalele care au atins criteriul de învățare au prezentat menținerea performanței cognitive, iar activitatea antiamnezică determinată a fost de 106,4%.

Keywords: synthesis, amides of 2-(3-(1-benzyl-5-oxopyrrolidin-3-yl)-5-thioxo-4,5-dihydro-1*H*-1,2,4-triazol-4-yl)acetic acid, docking studies, nootropic activity

Introduction

In recent decades, there has been an increase in the demand for nootropic drugs (1). This trend is associated with the spread of neurodegenerative diseases of various etiologies, accompanied by CNS disorders with a decrease in cognitive functions (2, 3). One of the factors of these disorders is traumatic brain injury. Unfortunately, in recent years, there has been an increase in the number of cases of injuries to military and civilians as a result of hostilities (4, 5). The COVID-19 pandemic has left a significant mark on the occurrence of brain disorders. As numerous studies have shown, this disease causes not only

acute respiratory disorders, but also has a long-term negative impact on the central nervous system (6). Among the undesirable effects are accelerated brain aging and decreased cognitive function, which are likely associated with increased neuroinflammation, oxidative stress, and impaired neuroplasticity (7).

A constant unstable nervous and psychological state catalyzes the process of brain aging, contributing to neurodegenerative processes leading to dementia (8, 9). As a result, it can occur much earlier, and the number of patients who have dementia may increase (10). Alzheimer's disease is completely incurable and has needed in-depth study and the search for new treatments for many years (11, 12). With the available drugs, it is only possible to reduce symptom manifestations, so it is not surprising that scientists are increasingly interested in research aimed at identifying an active molecule with a unique mechanism of action on memory (13-18).

A promising matrix for the rational design of biologically active compounds with nootropic effects is the 2-pyrrolidone core - a main scaffold that forms the basis of the racetam group of nootropics (19, 20). The rationale for seeking effective nootropics in this class of compounds is explained by the absence of adverse psychopharmacological effects (specifically sedation, analgesia, or motor or behavioral changes), unlike other classes of psychoactive drugs (21-25). It should be noted that the presence of an additional neuroprotective effect has expanded the practical use of racetams, namely, in the complex therapy of traumatic brain injuries, neuroinflammation, strokes, and encephalopathy of various etiologies (26-31). The range of indications for racetam use has become a focal point for directing scientific research. The evolution of the creation of racetam nootropics is based on modifying the structure of the first racetam drug, piracetam. Through the modification of the N-side chain and the introduction of substituents at position 4 of the pyrrolidin-2-one cycle, analogs of piracetam with better pharmacokinetic and safety profiles, as well as an expanded spectrum of pharmacological effects, have been created. In our opinion, this approach is justified and supported by scientific research and clinical application data (32). That is why the choice of an already existing nootropic racetam of the new generation for further modification will allow the creation of a potential series of derivatives with nootropic properties. 1-Benzyl-pyrrolidin-2-one is a structural fragment of the racetam nootropic nebracetam, whose modification with a 3-thio-1,2,4-triazole framework, saturated with heteroatom substituents, has led us to obtain promising compounds with nootropic activity (33). In our opinion, further modification of the structural framework of 1-benzyl-4-(5-sulfanylidene-4,5-dihydro-1H-1,2,4-triazol-3-yl)pyrrolidin-2-one may improve pharmacological properties, particularly increasing antiamnesic activity. One promising direction for further structural modification of the basic scaffold 4-(5-thioxo-4,5-dihydro-1H-1,2,4-triazol-3-yl)pyrrolidin-2-one is the incorporation of a molecular fragment, such as an acetic acid amide, into its structure. This choice is justified by the fact that some racetams contain a fragment of the acetic acid amide. For example, this includes the classic nootropic piracetam. It is this fragment of the molecule that is considered key to its ability to enhance the functioning of the central nervous system. Somewhat modified derivatives of piracetam – neofiracetam and phenylpiracetam – also retain the structural fragment of the acetic acid amide. Although in racetams this fragment is attached to the nitrogen atom of the pyrrolidone ring, in our series, we relocated it to the thiotriazole fragment to preserve the key pharmacophoric element and to evaluate the influence of its topological position on interactions with nootropic targets. Figure 1 shows the structural design of potential nootropic molecules.

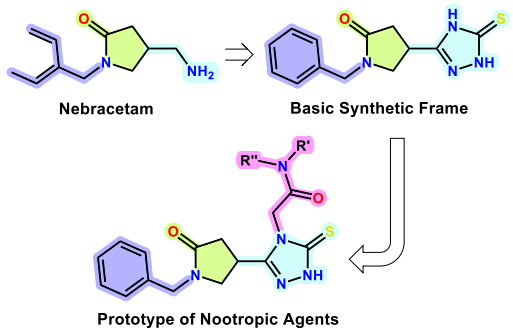

Figure 1.
Structural design of potential nootropic molecules

Materials and Methods

Analytical methods

Reagents manufactured by Sigma-Aldrich, USA, were used in this work. The required reagents were purified using standard techniques. Control of the reactions was carried out using thin-layer chromatography (eluent – ethyl acetate-hexane 1:2) on "Sorbfil UV-254" plates.

The elemental analysis was performed on a "Hewlett-Packard" automatic analyzer, M-180, by the company. ^{1}H NMR spectra were recorded on a Varian Gemini 400 MHz spectrometer and ^{13}C NMR spectra on a Varian Gemini 101 MHz spectrometer, both using DMSO-d6 as solvent. Chemical shifts are reported in δ (ppm) relative to residual solvent peaks. Coupling constants (J) are given in Hz, and multiplicities are described using standard abbreviations (s, d, t, q, m). LC/MS spectra were recorded on an Agilent 1100 LC/MSD SL system equipped with a diode array detector (G1315B, 3D) and a quadrupole mass detector (G1946B) operating in positive ESI mode. Chromatographic separation was

performed on a Zorbax SB-C18 Rapid Resolution HT cartridge (4.6 × 30 mm, 1.8 μm). The mobile phase consisted of A = H_2O + 0.1% HCOOH and B = MeCN + 0.1% HCOOH, using a linear gradient at a flow rate of 1.0 mL/min. The column temperature was maintained at 25 °C, and the injection volume was 5 μL.

Receptor-oriented flexible docking

The Autodock 4.2 software package was used for receptor-oriented flexible docking. Ligands were prepared using the MGL Tools 1.5.6 program (34). The Ligand optimization was performed using the Avogadro program. To perform calculations in Autodock 4.2, the receptor and ligand data were converted to a special PDBQT format. The nootropic effect has a complex mechanism that involves AMPA receptors and muscarinic (M1) acetylcholine receptors (35-37). The active macromolecular center of the nootropic targets (PDB IDs 3LSF and 6ZFZ) from the Protein Data Bank (PDB) was used as a biological target for docking. 3LSF B+E: coordinates x = 6.886, y = 53.146, z = 28.488, size x = 22, y = 26, z = 40; 6ZFZ A: coordinates x = 22.442, y = 20.533, z = -6.969, size x=24, y = 26, z = 24. The receptor maps were generated using the MGL Tools and AutoGrid programs. Water molecules, ions, and the ligand were removed from the PDB file. Visual analysis of the complexes of the tested molecules in the peptides' active sites, redocking visualization, and RMSD calculation were performed using the Discovery Studio Visualizer program.

Pharmacological study of antiamnestic activity

Justification of the amnesia model, selection of compounds for study, and comparison of drugs

An important component of the nootropic effect is antiamnestic action. Based on docking results, several synthesized compounds were evaluated for antiamnestic properties in a basic scopolamine-induced amnesia model in mice (33). Since this model is based on the disruption of cholinergic memory mechanisms, the selection of compounds was guided primarily by the docking results for the muscarinic (M1) acetylcholine receptor. On the other hand, it was important to limit the number of animal studies in accordance with bioethical principles. Therefore, 4 of the 12 synthesized compounds were selected for the pharmacological experiment: 9c, 9d, 9e, and 9i. Piracetam was used as a comparison drug at a dose of 300 mg/kg based on the chemical affinity to the synthesized substances and the proven antiamnestic effect (33).

Memory study method

To determine the effect of compounds on the processes of consolidation and recovery of memory engrams, the passive avoidance test (PAT) was used, as described in (33). The PAT is a widely used behavioral paradigm for assessing learning and memory. It is based on rodents' natural preference for dark environments and their ability to learn to avoid entering a dark compartment previously associated with an aversive stimulus (typically a mild foot shock). Memory retention is evaluated by measuring the latency to enter the dark compartment during the retention trial; longer latencies indicate better learning and memory performance. The PAT study device has two parts: an illuminated starting platform and a darkened chamber with an electrode floor. They are connected by an opening with a door. The study is conducted for two days. On the first day, the animals are trained. The mouse is placed on an illuminated platform with its tail facing the entrance to the dark chamber. The latency to entry into the dark compartment is determined, during which the animal is subjected to electrical stimulation at 0.6 mA. 24 h after this, the memory trace is tested: the latency time of entry is determined again. If the mouse does not enter the dark chamber within 3 min, it is considered to have reached the learning criterion (latency period is 180 s).

Modeling of amnesia and parameters of antiamnestic activity

Anterograde amnesia was modeled by the administration of scopolamine hydrobromide trihydrate (Thermo Fisher Scientific, China) at a dose of 1.5 mg/kg intraperitoneally (i.p.) (38). Scopolamine was administered 20 min before the formation of PAT (electropainful stimulation of the mouse paw). After 24 h, the latent period of entry of animals into the dark chamber and the number of animals that reached the learning criterion were re-determined. The index of antiamnestic activity (AA) was calculated using the modified Buttler formula (38):

$$AA = (\Delta TLD - \Delta TLAC) / (\Delta TLVC - \Delta TLAC) \times 100\ (\%),$$

AA – antiamnestic activity, %; ΔTLD – the change in latency of the training and retention test for the drug-treated group (substances or piracetam); ΔTLAC – the change in latency of the training and retention test for the scopolamine-treated group (amnesia control group); ΔTLVC – the change in latency of the training and retention test for the vehicle control group.

Also, during PAT testing, the number of unfinished attempts to enter the animal into the dark chamber (NUAE) was determined after 24 hours, which characterizes hesitation to enter (39). The animals are peeking into the dark compartment without full-body entry.

The study used 42 white male mice weighing 20 - 25 g. In accordance with the requirements of bioethics, a minimum number of animals of the same sex were used at the pharmacological screening stage to determine the presence of a mnemotropic effect of the tested compounds. The animals were obtained from the vivarium of the National Pharmaceutical

University (Kharkiv, Ukraine). The experiment was performed at the Educational and Scientific Institute of Applied Pharmacy of the National University of Pharmacy. The mice were kept at 22 - 23°C, 50% air humidity, a 12-hour light/dark cycle, and free access to food and water.

Animals were randomly divided into 7 groups of 6 animals each. Sample size *per* group was 6, based on previous studies (33) and effect size estimates (D = 2.0 - 2.5) (40). Group 1 – vehicle control (VC): animals that were administered intragastrically (i.g.) water 10 min before i.p. administration of 0.9% NaCl solution to standardize the experimental conditions. Group 2 – amnesia control (AC) animals were administered i.g. water, and after 15 min, amnesia was simulated by administering scopolamine 1.5 mg/kg i.p.; after 20 min, PAT was formed. Group 3 – animals that were administered the comparison drug piracetam (Farmak, Ukraine) 300 mg/kg i.g. (33), after 15 min, amnesia was simulated, and after 20 min, PAT was formed. Groups 4 - 7 – animals that were administered the test substances 15 min before amnesia simulation, and after the next 20 min, PAT was formed. Animals in groups 4 - 7 were administered i.g. aqueous suspensions of the investigated pyrrolidine derivatives, stabilized with Tween-80, at equimolar doses (87 - 100 mg/kg). The choice of this dose level is explained by the fact that they are about 1/10 of the LD50, which

was determined *in silico* for compounds of this series [33]. The volume of fluid administered, *i.e.*, was 0.1 ml *per* 10 g of body weight.

Ethical approval

All animal procedures were approved by the Bioethics Committee of the National University of Pharmacy, Ukraine (Approval No. 12/2024, protocol 10.01.2024). Experiments complied with the European Convention for the Protection of Vertebrate Animals (1986, revised 1998), Directive 2010/63/EU, and Ukrainian legislation (Law No. 3446-IV, 2006) (41).

Statistical analysis

Statistical analysis was performed using Statistica v. 12.0. The nature of the distribution was determined by the Shapiro-Wilk test. As the data were normally distributed, comparisons were made using ANOVA with post hoc Tukey's test. Results are presented as means ± standard error (M±SEM) and percentages. Categorical outcomes (number of animals that have reached the learning criterion) were evaluated by Fisher's angular transformation (φ). Differences were considered statistically significant at $p < 0.05$.

Results and Discussion

In order to obtain target amides 9 (a-l), a chemical modification of the scaffold 4-(5-thioxo-4,5-dihydro-1H-1,2,4-triazol-3-yl)pyrrolidin-2-one (33) that we previously obtained was carried out by introducing an acetic acid moiety and subsequent amidation with the corresponding amines (Figure 2). The first two stages of the synthesis are analogous to the previously described synthesis (33) and involve obtaining 1-benzyl-5-oxo-pyrrolidine-3-carboxylic acid 3 and the corresponding hydrazide 4. Further heating of hydrazide 4 with ethyl 2-isothio-cyanato-acetate 5 in methanol led to the formation of the intermediate thiosemicarbazide 6, which was cyclized into 2-[3-(1-benzyl-5-oxo-pyrrolidin-3-yl)-5-sulfonyliden-4,5-dihydro-1H-1,2,4-triazol-4-yl]acetic acid 7. Further amidation of acid 7 with the corresponding amines 8 (a-l) was carried out in the presence of carbonyldiimidazole (CDI) under heating in an anhydrous dioxane medium (Figure 1).

The synthesized amides of 2-(3-(1-benzyl-5-oxopyrrolidin-3-yl)-5-thioxo-4,5-dihydro-1H-1,2,4-triazol-4-yl)acetic acid 9 (a-l) are white precipitates, which are well soluble in 2-propanol, ethanol, methanol, dimethylformamide (DMF), and dimethyl sulfoxide (DMSO), and insoluble in water.

The structures and purities of the compounds obtained were confirmed by elemental analysis, 1H nuclear magnetic resonance (NMR) spectroscopy, and carbon-13 NMR spectroscopy.

(^{13}C NMR) spectroscopy and liquid chromatography mass spectrometry (LC/MS). The reaction was monitored by thin-layer chromatography.

General method of synthesis of amides of 2-(3-(1-benzyl-5-oxopyrrolidin-3-yl)-5-thioxo-4,5-dihydro-1H-1,2,4-triazol-4-yl)acetic acid 9 (a- l)

To benzylamine 1 (0.01 mol) was added itaconic acid 2 (0.01 mol) in DMF when heated to 180-200°C for 5 hours. The resulting precipitate was washed with ethanol and filtered. Further, CDI (0.011 mol) in dioxane was added to the obtained 1-benzyl-5-oxopyrrolidine-3-carboxylic acid 3, and then hydrazine hydrate in an equimolar ratio. The reaction mixture was stirred while heating to 80°C for 5 hours. The precipitate formed was filtered off, dried, and crystallized from ethanol. To 1-benzyl-5-oxopyrrolidine-3-carbohydrazide 4 (0.01 mol) in 50 ML of methanol with stirring, add 0.01 mol of 2-isothiocyanate acetic acid 5. The reaction mixture was heated to 60°C for 4 hours. Next, the reaction mixture is cooled, 100 mL of water is added, and the precipitate formed is filtered off and dried. The resulting intermediate thiosemicarbazide 6 is dissolved in water, heated to dissolution, and 0.15 mol of sodium hydroxide is added at 100°C for 3 hours. Then leave to cool to room temperature. After cooling, acidify the mixture with hydrochloric acid to pH = 6.5-7. The resulting 2-[3-(1-benzyl-5-oxo-pyrrolidin-3-yl)-5-sulfanylidene-4,5-dihydro-1*H*-1,2,4-triazol-4-yl]acetic acid 7 is filtered off and dried. To a 30% solution of acid 7 in dioxane, CDI (1.1 equiv.) was added portionwise. The reaction mixture was stirred for 3 h at room temperature, and the corresponding

amine 8(a-l) was added as a 50% dioxane solution. The mixtures are stirred for 5 hours, dioxane is distilled off on a rotary evaporator, and the residues are diluted with water and acidified with 0.1 M hydrochloric acid solution to pH=5-6. The final product precipitate 9(a-l) is filtered off and dried. Crystallization was carried out from 2-propanol. .

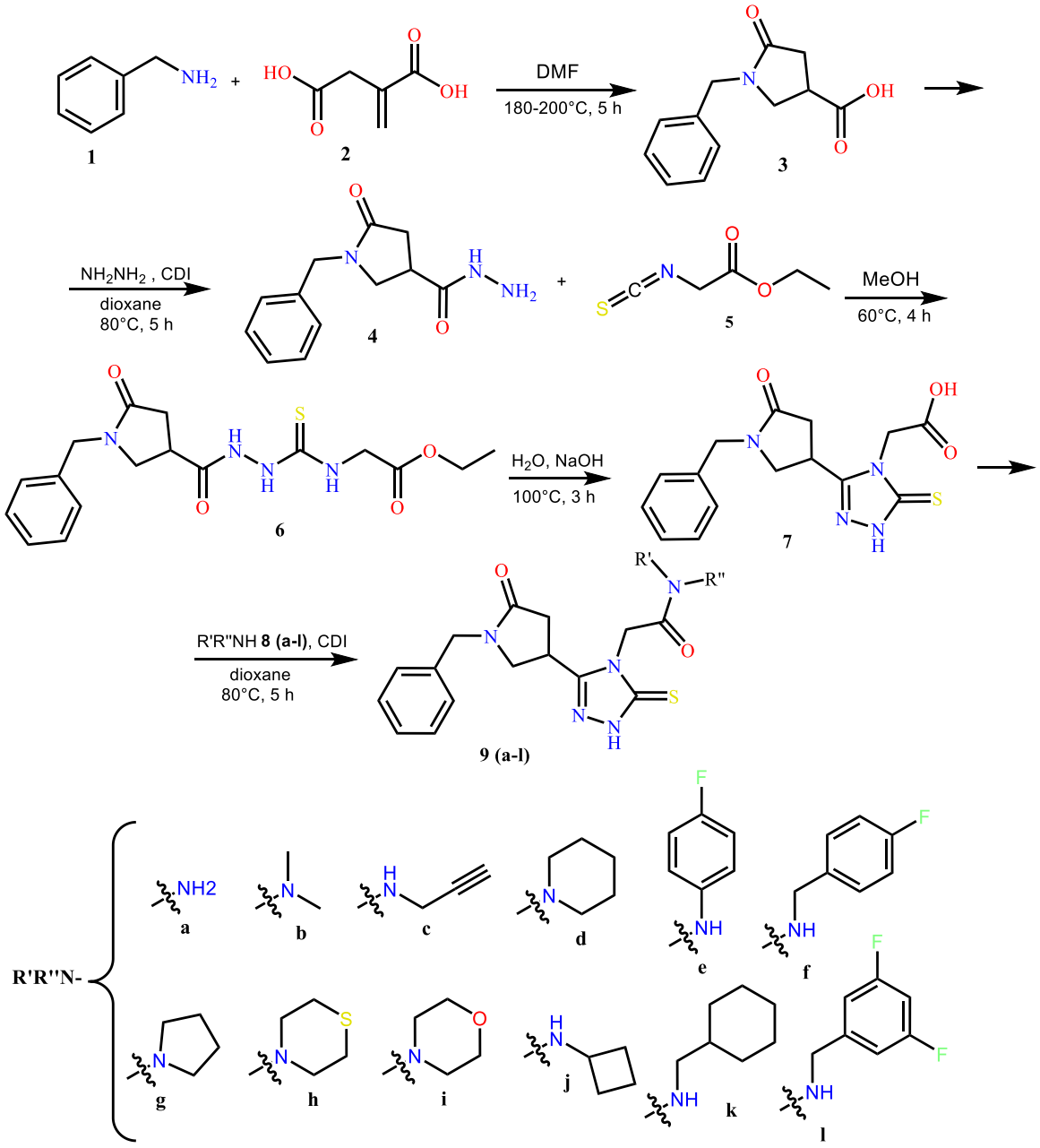

Figure 2.
Compound synthesis scheme (33)

2-[3-(1-Benzyl-5-oxopyrrolidin-3-yl)-5-sulfanylidene-4,5-dihydro-1H-1,2,4-triazol-4-yl]acetamide 9a

78% yield. ^{1}H NMR (400 MHz, DMSO-d$_6$) δ: 4.38 (s, 2H) (CH_2, 2H); 5.29 (s, 2H) (CH_2, 2H); 2.77-2.89 (m, 2H) (CH_2, 2H); 3.56 (t, J = 12 Hz, 1H), 3.62 (m, 2H), (-C<u>H$_2$</u>-C<u>H</u>-<u>CH$_2$</u>- 5H pyrrolidine); ArH+NH_2: 7.2 – 7.32 (m, 7H); 13.80 (s, 1H, NH- 1,2,4-triazole). ^{13}C NMR (100 MHz, DMSO-d$_6$) δ: 174.63, 173.24, 171.18, 153.85, 136.35, 128.38, 128.36, 127.82, 51.67, 47.50, 47.12, 35.89, 34.21. 21.13% N, 9.67% S, Calculated for $C_{15}H_{17}N_5O_2S$. Found,%: N 21.35, S 9.71. LC/MC m/z: 332.2 [$(M+H)^+$].

2-[3-(1-Benzyl-5-oxopyrrolidin-3-yl)-5-sulfanylidene-4,5-dihydro-1H-1,2,4-triazol-4-yl]-N,N-dimethylacetamide 9b

78% yield. ^{1}H NMR (400 MHz, DMSO-d$_6$) δ: 2.83 (s, 3H) (CH_3, 3H); 3.05 (s, 3H) (CH_3, 3H); 4.40 (s, 2H) (CH_2, 2H); 4.91 (s, 2H) (CH_2, 2H); 2.55-2.77 (m, 2H), 3.40 (t, J = 4.0 Hz, 1H), 3.51-3.60 (m, 2H),

(-C<u>H</u>$_2$-C<u>H</u>-C<u>H</u>$_2$- 5H pyrrolidine); ArH (5H): 7.21-7.23 (d, J = 7.2 Hz, 2H), 7.27-7.29 (m, 1H), 7.32-7.34 (m, 2H); 13.69 (s, 1H, NH- 1,2,4-triazole). ^{13}C NMR (100 MHz, DMSO-d$_6$) δ: 174.17, 172.76, 170.74, 152.86, 136.23, 128.23, 128.20, 127.55, 50.36, 47.22, 46.04, 35.89, 35.87, 34.59. 19.48% N, 8.92% S, Calculated for $C_{17}H_{21}N_5O_2S$. Found,%: N 19.71, S 9.15. LC/MC m/z: 360.2 [(M+H)$^+$].

2-[3-(1-Benzyl-5-oxopyrrolidin-3-yl)-5-sulfanylidene-4,5-dihydro-1H-1,2,4-triazol-4-yl]-N-(prop-2-yn-1-yl)acetamide 9c

78% yield. ^{1}H NMR (400 MHz, DMSO-d$_6$) δ: 4.39 (s, 2H) (CH$_2$, 2H); 4.91 (s, 2H) (CH$_2$, 2H); 2.32 (s, 1H), 2.59-2.6 (d, J = 4.0 Hz, 3H), 2.82-3.83 (d, J = 4.0 Hz, 1H), (-C<u>H</u>$_2$-C<u>H</u>-C<u>H</u>$_2$- 5H pyrrolidine); 3.91 (m, 1H), 4.05-4.06 (d, J = 4Hz, 2H) (prop-2-yn-1-yl); ArH: 7.25-7.36 (m, 5H); 8.24 (s, J = 5.6 Hz, 1H) (-CO-NH, 1H); 13.70 (s, 1H, NH- 1,2,4-triazole). ^{13}C NMR (100 MHz, DMSO-d$_6$) δ: 173.91, 172.76, 169.24, 153.29, 136.23, 128.23, 128.20, 127.55, 79.24, 72.30, 50.36, 47.22, 46.57, 35.89, 34.59, 30.74. 18.96% N, 8.68% S, Calculated for $C_{18}H_{19}N_5O_2S$. Found,%: N 19.12, S 8.92. LC/MC m/z: 370.2 [(M+H)$^+$].

1-Benzyl-4-{4-[2-oxo-2-(piperidin-1-yl)ethyl]-5-sulfanylidene-4,5-dihydro-1H-1,2,4-triazol-3-yl}pyrrolidin-2-one 9d

78% yield. ^{1}H NMR (400 MHz, DMSO-d$_6$) δ: 4.4 (dd, J = 12.4, 6.8 Hz, 2H) (CH$_2$, 2H); 4.93 (s, 2H) (CH$_2$, 2H); 1.32 (s, 2H), 1.53 (s, 4H), 3.30-3.32 (m, 3H), 3.63 (dd, J = 12.3, 6.8 Hz, 1H) (piperidine-2-yl, 10H); 2.52 (d, J = 7.0 Hz, 1H), 2.63(d, J = 7.0 Hz, 1H), 3.25-3.29 (m, 2H), 3.57-3.61 (m, 1H), (-C<u>H</u>$_2$-C<u>H</u>-C<u>H</u>$_2$-5H pyrrolidine); ArH: 7.21-7.23 (m, 2H), 7.27 (m, 1H), 7.32-7.34 (m, 2H); 13.70 (s, 1H, NH-1,2,4-triazole). ^{13}C NMR (100 MHz, DMSO-d$_6$) δ: 174.17, 172.76, 169.87, 152.89, 136.23, 128.23, 128.20, 127.55, 50.36, 47.22, 46.50, 45.65, 35.89, 34.58, 25.48, 24.23.

17.53% N, 8.02% S, Calculated for $C_{20}H_{25}N_5O_2S$. Found,%: N 17.71, S 8.21. LC/MC m/z: 400.2 [(M+H)$^+$].

2-[3-(1-Benzyl-5-oxopyrrolidin-3-yl)-5-sulfanylidene-4,5-dihydro-1H-1,2,4-triazol-4-yl]-N-(4-fluorophenyl)acetamide 9e

77% yield. ^{1}H NMR (400 MHz, DMSO-d$_6$) δ: 4.40 (s, 2H) (CH$_2$, 2H); 4.88 (s, 2H) (CH$_2$, 2H); 2.88 (s, 2H), 3.32-3.38 (m, 1H), 3.62 (t, 1H, 6.8 Hz), 3.7-3.8 (m, 1H) (-C<u>H</u>$_2$-C<u>H</u>-C<u>H</u>$_2$- 5H pyrrolidine); ArH: 7.16 (t, 2H, J = 8.8 Hz), 7.22 and 7.27 (dd, 3H, J = 7.2 Hz), 7.31-7.35 (m, 2H), 7.55-7.58 (m, 2H); 10.5 (s, 1H) (-CO-NH, 1H); 13.70 (s, 1H, NH- 1,2,4-triazole). ^{13}C NMR (100 MHz, DMSO-d$_6$) δ: 174.04, 172.76, 166.90, 159.26, 156.80, 152.96, 136.23, 135.14, 135.11, 128.23, 128.20, 127.55, 121.68, 121.60, 115.59, 115.37, 50.36, 47.22, 47.02, 35.89, 34.62. 16.46% N, 7.53% S, Calculated for $C_{21}H_{20}FN_5O_2S$. Found,%: N 16.72, S 7.78. LC/MC m/z: 426.0 [(M+H)$^+$].

2-[3-(1-Benzyl-5-oxopyrrolidin-3-yl)-5-sulfanylidene-4,5-dihydro-1H-1,2,4-triazol-4-yl]-N-[(4-fluorophenyl)methyl]acetamide 9f

76% yield. ^{1}H NMR (400 MHz, DMSO-d$_6$) δ: 4.40 (d, J = 4 Hz, 2H), 4.64-4.72 (q, J = 12 Hz, 2H), 4.95 (s, 2H) (3×CH$_2$, 6H); 2.59-2.64 (dd, J = 4, 8 Hz, 1H), 2.82-2.87 (dd, J = 4, 8 Hz, 1H), 3.68-3.77 (mddd, J = 12, 8, 4 Hz, 2H), 3.87-3.91 (m, 1H) (-C<u>H</u>$_2$-C<u>H</u>-C<u>H</u>$_2$- 5H pyrrolidine); ArH: 7.11-7.16 (м, 1H), 7.23-7.38 (м, 8H); 9.53 (t, *J* = 5.5 Hz, 1H) (-CO-NH, 1H); 13.68 (s, 1H, NH- 1,2,4-triazole). ^{13}C NMR (100 MHz, DMSO-d$_6$) δ: 173.91, 172.76, 169.20, 163.27, 160.81, 153.25, 136.23, 135.32, 135.29, 129.49, 129.40, 128.23, 128.20, 127.55, 115.23, 115.01, 50.36, 47.22, 46.62, 43.33, 35.89, 34.59. 15.93% N, 7.29% S, Calculated for $C_{22}H_{22}FN_5O_2S$. Found,%: N 16.12, S 7.41. LC/MC m/z: 440.2 [(M+H)$^+$].

1-Benzyl-4-{4-[2-oxo-2-(pyrrolidin-1-yl)ethyl]-5-sulfanylidene-4,5-dihydro-1H-1,2,4-triazol-3-yl}pyrrolidin-2-one 9g

77% yield. ^{1}H NMR (400 MHz, DMSO-d$_6$) δ: 4.35-4.42 (q, J = 12 Hz, 2H) (CH$_2$, 2H); 4.91 (s, 2H) (CH$_2$, 2H); 1.86 (t, J = 12 Hz 4H), 3.33 (s, 4H) (pyrrolidine-1-yl, 8H); 2.59-2.64 (dd, J = 12.4, 7.0 Hz, 1H), 2.82 (dd, J = 12.4, 6.9 Hz, 1H), 3.68-3.71 (m, 2H), 3.75-3.77 (m, 1H), (-C<u>H</u>$_2$-C<u>H</u>-C<u>H</u>$_2$- 5H pyrrolidine); ArH: 7.23-7.36 (m, 5H); 13.65 (s, 1H, NH- 1,2,4-triazole).^{13}C NMR (100 MHz, DMSO-d$_6$) δ: 174.17, 172.76, 171.60, 152.89, 136.23, 128.23, 128.20, 127.55, 50.36, 47.22, 46.50, 46.48, 35.89, 34.58, 24.82. 18.17% N, 8.32% S, Calculated for $C_{19}H_{23}N_5O_2S$. Found,%: N 18.25, S 8.48. LC/MC m/z: 386.1 [(M+H)$^+$].

1-Benzyl-4-{4-[2-oxo-2-(thiomorpholin-4-yl)ethyl]-5-sulfanylidene-4,5-dihydro-1H-1,2,4-triazol-3-yl}pyrrolidin-2-one 9h

78% yield. ^{1}H NMR (400 MHz, DMSO-d$_6$) δ: 4.4 (q, J = 14.8 Hz) (CH$_2$, 2H); 4.94 (s, 2H) (CH$_2$, 2H); 3.38-3.41 (m, 1H), 3.5-3.8 (m, 7H) (thiomorpholin-4-yl, 8H); 2.5 (d, J = 2 Hz, 1H), 2.54-2.78 (m, 3H), 3.4 (dd, J = 4, 3.8 Hz, 1H) (-C<u>H</u>$_2$-C<u>H</u>-C<u>H</u>$_2$- 5H pyrrolidine); ArH: 7.22-7.24 (m, 2H), 7.28-7.29 (d, J = 8 Hz, 1H), 7.32-7.36 (m, 2H); 13.62 (s, 1H, NH-1,2,4-triazole). ^{13}C NMR (100 MHz, DMSO-d$_6$) δ: 174.17, 172.76, 169.72, 152.89, 136.23, 128.23, 128.20, 127.55, 50.36, 47.22, 46.94, 46.53, 35.89, 34.58, 27.76. 16.77% N, 15.36% S, Calculated for $C_{19}H_{23}N_5O_2S_2$. Found,%: N 16.91, S 15.48. LC/MC m/z: 418.1 [(M+H)$^+$].

1-Benzyl-4-{4-[2-(morpholin-4-yl)-2-oxoethyl]-5-sulfanylidene-4,5-dihydro-1H-1,2,4-triazol-3-yl}pyrrolidin-2-one 9i

75% yield. ^{1}H NMR (400 MHz, DMSO-d$_6$) δ: 4.4 (q, J = 14.8 Hz) (CH$_2$, 2H);

4.95 (s 2H) (CH$_2$, 2H); 3.50-3.55 (m, 5H), 3.59-3.63 (m, 3H), (morpholin-4-yl, 8H); 2.5 (d, J = 5.6 Hz,

1H), 2.74 (dd, J = 12.5, 6.9 Hz, 1H), 3.34-3.41 (m, 3H) (-C<u>H</u>$_2$-C<u>H</u>-C<u>H</u>$_2$- 5H pyrrolidine); ArH: 7.21-7.23 (d, J = 5.6 Hz, 2H), 7.27-7.29 (d, J = 6.8 Hz, 1H), 7.32-7.36 (m, 2H); 13.70 (s, 1H, NH- 1,2,4-triazole). ^{13}C NMR (100 MHz, DMSO-d$_6$) δ: 174.17, 172.76, 169.81, 152.89, 136.23, 128.23, 128.20, 127.55, 66.38, 50.36, 47.22, 46.47, 44.78, 35.89, 34.58. 17.44% N, 7.99% S, Calculated for $C_{19}H_{23}N_5O_3S$. Found,%: N 17.65, S 8.12. LC/MC m/z: 402.0 [(M+H)$^+$].

2-[3-(1-Benzyl-5-oxopyrrolidin-3-yl)-5-sulfanylidene-4,5-dihydro-1H-1,2,4-triazol-4-yl]-N-cyclobutylacetamide 9j

78% yield. ^{1}H NMR (400 MHz, DMSO-d$_6$) δ: 4.34 (q, J = 1.3 Hz) (CH$_2$, 2H); 4.92 (s 2H) (CH$_2$, 2H); 1.52-1.61 (m, 1H), 1.8-1.94 (m, 6H), (cyclobutyl, 7H); 2.59-2.64 (dd, J = 4, 8 Hz, 1H), 2.82-2.87 (dd, J = 4, 8 Hz, 1H), 3.67-3.78 (m, 2H), 3.87-3.93 (m, 1H) (-C<u>H</u>$_2$-C<u>H</u>-C<u>H</u>$_2$- 5H pyrrolidine); ArH: 7.20-7.38 (m, 5H); 8.43 (d, J = 7.5 Hz, 1H), (-CO-NH, 1H); 13.66 (s, 1H, NH- 1,2,4-triazole). ^{13}C NMR (100 MHz, DMSO-d$_6$) δ: 173.91, 172.76, 169.44, 153.25, 136.23, 128.23, 128.20, 127.55, 50.36, 49.09, 47.22, 46.85, 35.89, 34.59, 31.28, 18.29. 18.17 % N, 8.32 % S, Calculated for $C_{19}H_{23}N_5O_2S$. Found,%: N 18.35, S 8.43. LC/MC m/z: 386.2 [(M+H)$^+$].

2-[3-(1-Benzyl-5-oxopyrrolidin-3-yl)-5-sulfanylidene-4,5-dihydro-1H-1,2,4-triazol-4-yl]-N-(cyclohexylmethyl)acetamide 9k

75% yield. ^{1}H NMR (400 MHz, DMSO-d$_6$) δ: 3.02 (dd, *J* = 6.0, 4.6 Hz, 2H) (CH$_2$, 2H); 4.38 (q, J = 12 Hz) (CH$_2$, 2H); 4.91 (s 2H) (CH$_2$, 2H); 1.20-1.57 (m, 10H), 1.65-1.7 (m, 1H), (cyclohexyl, 11H); 2.59-2.64 (dd, J = 4, 8 Hz, 1H), 2.82-2.87 (dd, J = 4, 8 Hz, 1H), 3.67-3.78 (m, 2H), 3.87-3.91 (m, 1H) (-C<u>H</u>$_2$-C<u>H</u>-C<u>H</u>$_2$- 5H pyrrolidine); ArH: 7.23-7.36 (m, 5H); 8.80 (t, J = 4 Hz, 1H), (-CO-NH, 1H); 13.64 (s, 1H, NH- 1,2,4-triazole). ^{13}C NMR (100 MHz, DMSO-d$_6$) δ: 173.91, 172.76, 170.17, 153.25, 136.23, 128.23, 128.20, 127.55, 50.36, 47.22, 46.73, 44.56, 36.81, 35.89, 34.59, 30.53, 26.54, 25.68. 16.38 % N, 7.50 % S, Calculated for $C_{22}H_{29}N_5O_2S$. Found,%: N 16.85, S 7.78. LC/MC m/z: 428.2 [(M+H)$^+$].

2-[3-(1-Benzyl-5-oxopyrrolidin-3-yl)-5-sulfanylidene-4,5-dihydro-1H-1,2,4-triazol-4-yl]-N-[(3,5-difluorophenyl)methyl]acetamide 9l

78% yield. ^{1}H NMR (400 MHz, DMSO-d$_6$) δ: 4.55 (d, *J* = 4Hz, 2H) (CH$_2$, 2H); 4.34-4.42 (dd, J = 16, 12 Hz) (CH$_2$, 2H); 4.93 (s 2H) (CH$_2$, 2H); 2.59-2.64 (dd, J = 4, 4 Hz, 1H), 2.82-2.87 (dd, J = 4, 8 Hz, 1H), 3.67-3.70 (m, 1H), 3.73-3.78 (m, 1H), 3.87-3.91 (m, 1H) (-C<u>H</u>$_2$-C<u>H</u>-C<u>H</u>$_2$- 5H pyrrolidine); ArH: 6.9-6.94 (q, J = 4 Hz, 1H), 6.96-6.97 (m, 1H) 7.02-7.05 (d, J = 12 Hz, 1H), 7.23-7.36 (m, 5H); 9.73-9.76 (m, 1H), (-CO-NH, 1H); 13.67 (s, 1H, NH- 1,2,4-triazole). ^{13}C NMR (100 MHz, DMSO-d$_6$) δ: 173.91, 172.76, 169.22, 164.65, 164.48, 162.18, 162.01, 153.25, 141.70, 141.60, 141.49, 136.23, 128.23, 128.20, 127.55, 112.00, 111.96, 111.79, 111.74, 102.94, 102.68, 102.43, 50.36, 47.22, 46.62, 43.58, 43.52, 43.46, 35.89, 34.59.

15.31 % N, 7.01 % S, Calculated for $C_{22}H_{21}F_2N_5O_2S$. Found,%: N 15.78, S7.43. LC/MC m/z: 458.2 [(M+H)$^+$].

«Drug-like» properties and molecular docking

For the tested molecules, the parameters of «drug-like» properties were calculated to assess compliance with Lipinski's rule, and an analysis was performed using the software pkSCM (Table I).

Table I

Predictive «drug-like» and ADMET properties

№	Descriptor						Permeability	
	MW	**RotB**	**Log P**	**nOHNH**	**nON**	***tPSA***	**BBB**	**CNS**
9a	331.4	5	-0.42	3	7	131.02	-0.953	-3.010
9b	359.45	5	-0.69	1	7	132.87	-0.957	-3.756
9c	369.45	6	0.63	2	7	183.02	-0.953	-3.433
9d	399.51	5	1.10	1	7	162.00	-1.195	-3.113
9e	425.48	7	0.73	2	7	171.89	-0,811	-3.063
9f	439,51	7	0.41	2	7	178.20	-0.751	-3.232
9g	385,49	5	0,16	1	7	162.80	-0.605	-3.531
9h	417.56	5	0.14	1	7	172.90	-0.672	-3.563
9i	401.49	5	1.67	1	8	167.47	-0.700	-3.767
9j	385,48	5	-0.91	3	8	162.31	-0.608	-3.394
9k	427,56	7	-0.76	3	8	95.31	-0.534	-3.111
9l	457.50	7	-1.40	3	8	95.31	-0.948	-3.263

molecular weight (MW), rotatable bond (RotB), lipophilicity coefficient (Log P), number of hydrogen bond donors (nOHNH), number of hydrogen bond acceptors (nON), topological polar surface area (tPSA), permeability brain blood barrier (BBB), permeability central nervous system (CNS)

Testing of the synthesized compounds showed that they all comply with Lipinski's rules. Penetration through the blood–brain barrier (BBB), expressed as log BB (ranging from –1.195 to –0.534), indicates that the compounds can cross the BBB, although partially limited, *i.e.*, they may moderately enter the brain *via* passive diffusion. The central nervous system (CNS) permeability parameter (log PS)

characterizes the permeability of brain capillary endothelial membranes. A range from –2 to –3 represents a moderate level for small organic molecules with average penetration. The remaining compounds, which show significantly more negative values, are likely to face the greatest barriers to CNS access. However, this does not exclude potential effects at sufficient doses or transporter involvement.

According to *in silico* analysis, all studied molecules show no signs of pronounced toxicity based on basic structural and pharmacological criteria. None of the compounds contains structural fragments associated with mutagenicity, carcinogenicity, or reproductive toxicity, indicating the absence of toxicophores in their molecular structures.

Another important indicator is the absence of PAINS alerts in all molecules. This means that the studied compounds are unlikely to yield false-positive results in biological tests and will not exhibit nonspecific activity. Similarly, the absence of Brenk alerts indicates the chemical stability of the molecules and a low propensity for unwanted reactions with biological macromolecules.

The potential risks associated with compounds are exclusively related to CYP450 enzyme inhibition, which is typical of many drugs and is not considered a critical factor in the early stages of development.

An informational assessment of the «drug-like» properties and pharmacokinetic profile of the studied compounds showed that they have favorable characteristics and can be recommended for further molecular docking.

Molecular docking of the synthesized compounds was carried out against the muscarinic (M1) acetylcholine receptor and AMPA receptor (PDB ID: 6ZFZ, 3LSF) at well-documented ligand-binding sites (35, 36). The replacement of the NMDA target with the AMPA receptor in our previous studies (33) was based on current evidence highlighting the role of AMPA receptors in cognitive processes and the mechanisms of action of nootropic agents. Many racetams (including piracetam, aniracetam, and oxiracetam) exert their activity primarily by modulating AMPA receptors, thereby enhancing synaptic transmission and memory (42). Therefore, selecting the AMPA receptor as a target is more justified for modeling potential nootropic compounds.

Based on their chemical structures, the substances under investigation are molecular hybrids of nebracetam, which has an agonistic mechanism of action at the muscarinic (M1) acetylcholine receptor (37). Therefore, he was also selected for redocking, in addition to the co-crystallized agonist 77LH281 (36). Considering the target compounds' classification as pyrrolidone nootropics, most of them, particularly the reference drug piracetam, modulate the AMPA receptor *via* positive allosteric modulation (35). In this regard, a redocking was performed for it relative to the chosen target. Despite the availability of crystallographic models of these receptors with co-crystallized ligands, the mechanism of action of racetam nootropics has not been definitively established; therefore, re-docking of reference molecules was conducted for two targets. In the AMPA receptor crystal, piracetam occupies multiple positions along the dimer interface, existing as several conformers with low electron density, indicating partial occupancy and molecular flexibility. This reflects its low affinity and weak binding stability, consistent with the millimolar K_i value (35). Therefore, for redocking, both the main ligand and the piracetam conformer were used. The obtained evaluation values from the re-docking (scoring function, free energy, and binding constant) were used as standards (Table II). The redocked native ligand structures showed similar orientations and binding positions in the active site region in relation to the crystallized native ligand structures with RMSD values ≤ 2 Å. (Piracetam (3LSF) – 1.0432 Å; piracetam conformer (3LSF) 0.9523 Å; ligand77LH281 (6ZFZ) 1.2306 Å. The ligand poses and binding site areas were determined correctly, as shown in Figure 3 (a-c).

The synthesized compounds and the comparison drug nebracetam contain an asymmetric carbon atom; thus, they can exist as enantiomers R and S (Figure 4). The molecular configuration is critical for ligand-receptor interaction; therefore, appropriate conformations of the enantiomers were generated, taking into account the correspondence of the chiral centers.

As a result of the docking, the best affinity of the studied molecules in enantiomeric configurations (R and S) was observed towards the muscarinic target rather than the AMPA receptor (Table II). As shown in the calculations, all tested molecules have moderate affinity for the AMPA receptor, with estimated values higher than those of piracetam but not exceeding the absolute values of nebracetam (Table II).

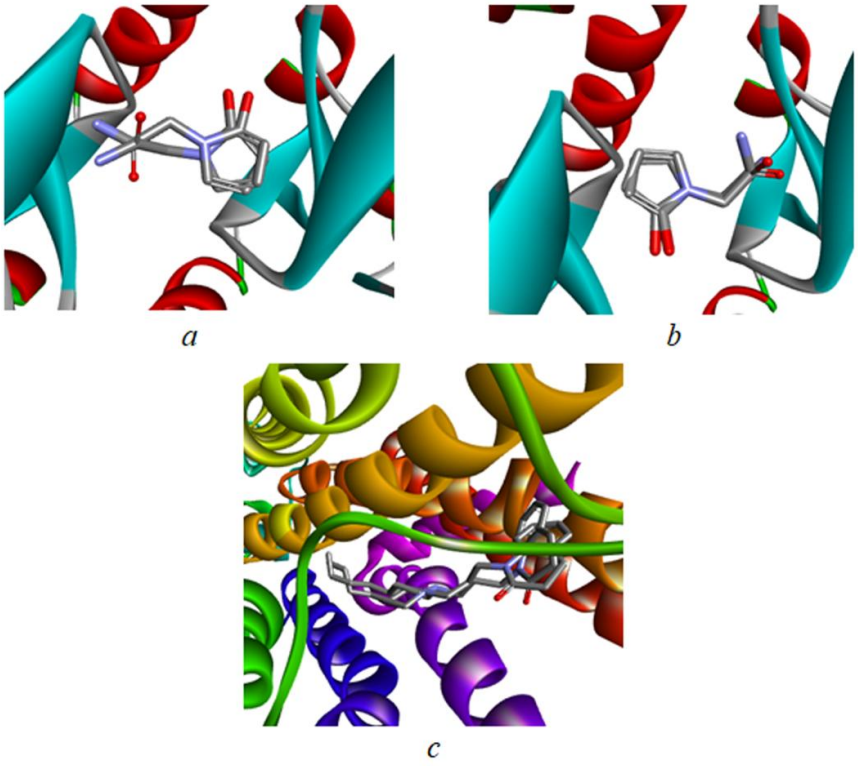

Figure 3.
Superimposed co-crystalized and re-docking native ligand in active site of biotarget: *a* – piracetam against AMPA receptor, *b* – piracetam conformer against AMPA receptor, *c* – ligand77LH281 against muscarinic (M1) acetylcholine receptor

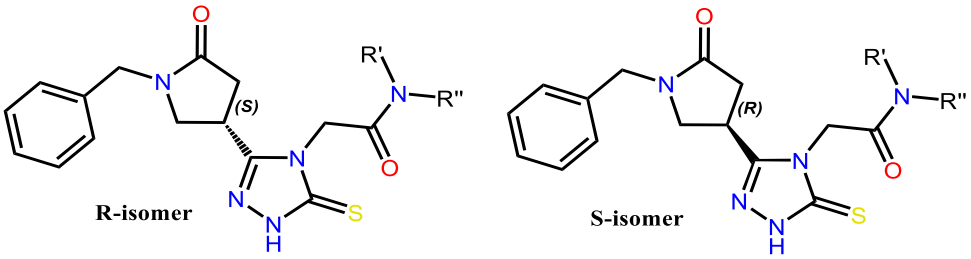

Figure 4.
R- and S- stereoisomers of synthesized derivatives 9 (a-l)

Table II
The values of Affinity DG, free binding energy, and binding coefficients for the best conformational positions of the test compound in combination with AMPA receptor (PDB ID: 3LSF) and muscarinic acetylcholine receptor (PDB ID: 6ZFZ)

Molecule		AMPA receptor			Muscarinic acetylcholine receptor		
		Affinity DG*	EDoc*	Ki µM *	Affinity DG*	EDoc*	Ki µM *
9a	R	-6.1	-4.39	605.37	-8.7	-6.36	21.63
	S	-7.1	-5.66	71.54	-9.5	-6.79	10.51
9b	R	-6.7	-5.65	71.66	-8.4	-7.07	6.52
	S	-6.9	-4.51	498.43	-8.6	-6.73	11.59
9c	R	-6.8	-5.47	98.27	-8.7	-7.15	5.75
	S	-7.0	-4.77	320.19	-10.0	-7.04	6.90
9d	R	-7.0	-4.18	862.73	-9.8	-8.15	1.06
	S	-7.3	-5.91	46.83	-9.6	-7.41	3.68
9e	R	-7.6	-4.48	517.01	-10.3	-7.76	2.05
	S	-9.0	-5.51	91.34	-9.9	-7.38	3.86
9f	R	-7.4	-4.53	477.82	-10.1	-6.08	34.75
	S	-7.7	-5.36	117.75	-10.4	-7.49	3.22

Molecule		AMPA receptor			Muscarinic acetylcholine receptor		
		Affinity DG*	EDoc*	Ki μM *	Affinity DG*	EDoc*	Ki μM *
9g	R	-6.9	-5.07	193.77	-9.1	-7.37	3.94
	S	-7.2	-5.42	106.88	-10.3	-7.53	3.00
9h	R	-6.5	-4.84	282.33	-9.5	-7.80	1.90
	S	-7.2	-5.55	85.47	-8.7	-7.00	7.36
9i	R	-7.0	-5.72	63.96	-9.6	-7.52	3.09
	S	-7.1	-5.85	51.39	-8.8	-7.04	6.97
9j	R	-6.7	-4.71	352.73	-9.1	-6.67	12.99
	S	-7.1	-4.85	279.32	-8.6	-6.83	9.83
9k	R	-6.9	-4.57	450.11	-10.3	-6.35	22.01
	S	-7.3	-4.29	717.75	-10.0	-6.86	9.32
9l	R	-8.5	-4.47	532.85	-10.2	-7.61	2.63
	S	-7.5	-4.76	324.90	-10.5	-5.99	40.51
Ne-brace-tam	R	-7.2	-5.79	56.93	-7.6	-6.63	13.92
	S	-6.2	-5.68	68.80	-7.5	-6.46	18.49
Piracetam		-5.3 -5.5**	-3.88 -4.02**	1430 1140**	-5.6	-3.59	2320
ligand77LH281					-9.0	-7.63	2.57

* Affinity DG, kcal/mol; *EDoc kcal/mol; *Ki μM micromolar; ** Estimated values for the piracetam conformer

According to the obtained data, the tested molecules had higher activity towards the M1 receptor than the reference drugs nebracetam and piracetam. Among the investigated molecules, the lead molecule 9d was proposed for further experimental screening, as it showed greater affinity for the M1 receptor than the co-crystallized agonist 77LH281 (Table II).

Figure 5 (a-b) shows the superpositions of the enantiomers *R* and *S* of the compound leader 9d in the active site of the muscarinic (M1) receptor compared to the co-crystallized ligand.

Based on the docking visualization, the nootropic effect is likely mediated by both configurations, as indicated by the binding modes relative to the agonist ligand. As seen in Figure 5 (a-b), the R-enantiomer, unlike the S-isomer, which is characterized by a typical binding mode of agonists, has proximity to the site of positive allosteric modulation, specifically the extracellular vestibule. The formation of a complex between the R-isomer and a network of hydrophobic amino acid residues mediates a conformational rearrangement in the extracellular vestibule, thereby causing its contraction and receptor activation (43, 44). Despite the presence of an unfavorable donor–donor interaction observed during the visualization of the ligand–target complex (Figure 5 (c-d)), the calculated docking energy values were the best among the studied molecules (Table I). This suggests that, under the modeling conditions, the likelihood of these repulsive forces significantly affecting the stability of the complex and its affinity for the receptor is low.

In addition to molecule 9d, the compounds 9c, 9e, and 9i (Table I) also had the most energetically favorable positions at the M1 receptor among the studied molecules, with high and medium computed docking values for both the R and S enantiomers. They were also selected for pharmacological screening.

Thus, the results of molecular docking not only allowed the identification of potential molecules for pharmacological screening but also guided pharmacological research in selecting the appropriate model for testing nootropic activity, in light of a probable agonistic effect on the muscarinic (M1) acetylcholine receptor. At the same time, the screening results indicate the effectiveness of predicting pharmacological effects using molecular docking.

Pharmacological screening

The results of pharmacological screening show (Table III) that the M-cholinoblocker scopolamine significantly impaired learning ability. All animals in the VC group reached the learning criterion (did not enter the dark chamber).

The number of mice in the AC group that reached the learning criterion decreased from 100% to 33.3% ($p < 0.01$ compared to VC). Also, in the AC group, NUAE significantly increased (up to 4.17 *per* animal, 5 times compared to VC, $p < 0.05$), indicating greater uncertainty when deciding to enter the dark chamber.

Piracetam caused a characteristic positive mnemotropic effect: 83.3% of animals reached the learning criterion ($p < 0.05$ compared to AC), while NUAE decreased compared to the AC group by 1.56 times, and AA was 49.4%.

Compound 9c caused an anti-amnestic effect at the level of piracetam: 83.3% of mice that had reached the learning criterion ($p < 0.05$ compared to AS), NUAE averaged 2.67 *per* animal, and AA was 46.5%.

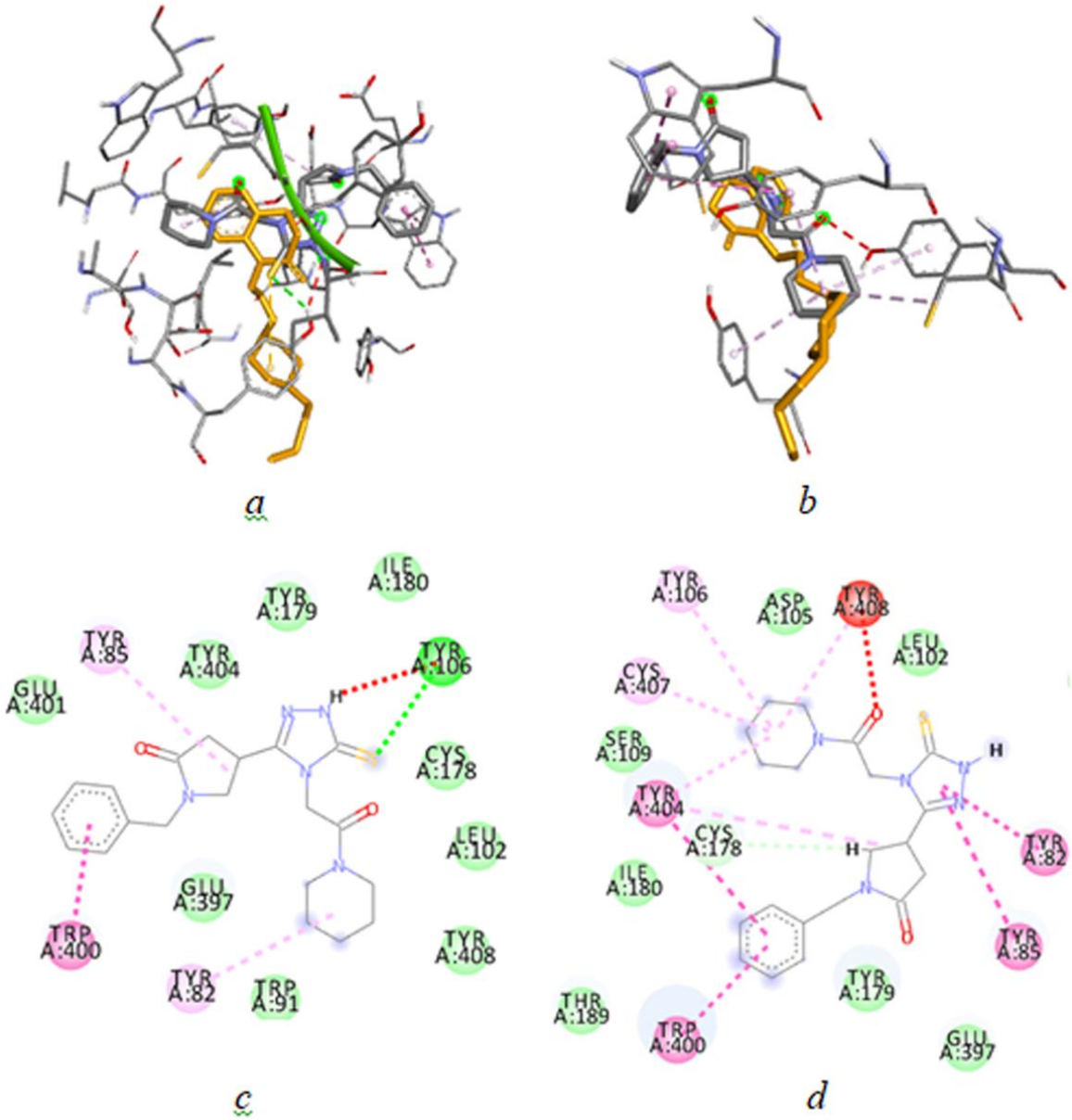

Figure 5.
Docking of molecule 9d (gray) and ligand 77LH281 (orange) in the active site of M1 muscarinic receptor: superposition of R and S enantiomers (a, b) and their intermolecular interaction diagrams (c, d)

Compound 9d emerged as the absolute leader in the screening. 100% of animals that have reached the learning criterion, as did mice from the VC group ($p < 0.01$ with respect to AS). NUAE decreased on average to 2.00 *per* animal and did not differ significantly from the VC group. At the same time, AA was 106.4%.

Compound 9e showed no antiamnestic effect. The learning criterion was reached by 66.7% of animals, *i.e.*, fewer than in VC ($p < 0.05$). NUAE was, on average, 2.33 *per* mouse, and AA was only 6.7.

Compound 9i turned out to be an outlier in the screening. It slightly increased the latency to entry after 24 h and did not affect the number of animals that reached the learning criterion (as in AS, this number was 33.3%). NUAE decreased compared to AS to 2.17 *per* mouse, and AA had a negative value (–47.1).

It is known that racetams can enhance cholinergic neurotransmission, particularly that mediated by M-cholinergic receptors, and also act as allosteric modulators of AMPA receptors (35, 37). Comparison of the results of pharmacological screening and molecular docking shows that the absolute leader of the screening, compound 9d, has the minimum Ki values for both receptors (M-cholinergic receptor and AMPA receptor) for the S enantiomer. *In vivo* studies in mice confirmed the predicted neurotropic potential of the investigated compounds, as predicted by molecular docking results.

Table III

The effect of substances on mice with scopolamine-induced amnesia in the passive avoidance test (M ± SEM)

Group, n	Transfer latency, sec			Number of animals that have reached the learning criterion		The number of unfinished attempts to enter (in 24 h)	AA, %
	training (1st day)	retention test (in 24 h)	difference	absolute	%		
Vehicle control (VC) (n = 6)	38.50 ± 6.25	180.00 ± 0.00	141.50 ± 6.25	6/6	100	0.83 ± 0.65	–
Amnesia control (AC) (n = 6)	68.83 ± 15.54	153.00 ± 14.59*	84.16 ± 15.23*	2/6	33.3**	4.17 ± 1.01*	–
Piracetam, 300 mg/kg (n = 6)	47.17 ± 13.08	159.66 ± 20.33	112.50 ± 20.10	5/6	83.3#	2.67 ± 0.49*	49.4
Substance **9c**, 87 mg/kg (n = 6)	41.67 ± 8.16	152.50 ± 27.50	110.83 ± 28.17	5/6	83.3#	2.67 ± 1.08	46.5
Substance **9d**, 94 mg/kg (n = 6)	34.83 ± 3.60	180.00 ± 0.00 #	145.17 ± 3.60 ##	6/6	100##	2.00 ± 0.82	106.4
Substance **9e**, 100 mg/kg (n = 6)	47.33 ± 9.59	135.33 ± 29.58	88.00 ± 23.91*	4/6	66.7*	2.33 ± 0.76	6.7
Substance **9i**, 94 mg/kg (n = 6)	41.17 ± 8.36	98.33 ± 34.80*	57.17 ± 28.91*	2/6	33.3**&	2.17 ± 0.98	–47.1

Notes: n – number of animals; AA – antiamnestic activity; * – $p < 0.05$; ** – $p < 0.01$ when compared with vehicle control; # – $p < 0.05$, ## – $p < 0.01$ when compared with amnesia control; & – $p < 0.05$ when compared with piracetam

Despite the absence of *in vitro* confirmation, the observed biological effects were consistent with computational predictions, as compound 9d completely abolished the scopolamine-induced amnesic effect in the *in vivo* experiment. However, no regularities of the relationship between these parameters are observed. For example, compound 9c, which showed AA at the level of piracetam, has a high Ki value for the M-cholinergic receptor and a low Ki value for the AMPA receptor. The outsider 9i has almost the same Ki value for the M-cholinergic receptor as 9c, but a low Ki value for the AMPA receptor, which is close to the leader 9d. The complexity of the nootropic effect mechanism can explain this. In particular, pyrrolidine nootropics can affect the above-mentioned targets and cause vasodilation in the hippocampus, thereby increasing nutrient and oxygen delivery to neurons (45). The combination of docking results and pharmacological screening confirms that the nootropic mechanism is polytropic. Compound 9d should be considered promising for further in-depth studies of the nootropic effect and its mechanisms.

The study has limitations

In particular, the assessment of the dose-response pattern for compound 9d, determination of the ED50 and maximum effect, elucidation of possible sex differences in the mnemotropic effect of the lead compound, and other aspects of its nootropic activity will be the tasks of further research.

Conclusions

New potential nootropic substances, amides of 2-(3-(1-benzyl-5-oxopyrrolidin-3-yl)-5-thioxo-4,5-dihydro-1H-1,2,4-triazol-4-yl)acetic acid, were synthesized. The structure and purity of the obtained substances were confirmed by elemental analysis, ^{1}H NMR, ^{13}C NMR spectroscopy, and LC/MS. From docking studies, potential molecules for experimental screening were identified, and recommendations were provided for selecting an appropriate model for nootropic activity, given the probable agonistic effect on the muscarinic (M1) acetylcholine receptor. The nootropic (anti-amnestic) activity of the synthesized substances was studied at the PJSC in a model of scopolamine amnesia in mice. As a result of experimental studies, the most promising hit compound 1-benzyl-4-{4-[2-oxo-2-(piperidin-1-yl)ethyl]-5-sulfanylidene-4,5-dihydro-1H-1,2,4-triazol-3-yl}pyrrolidin-2-one 9d was identified, which eliminated the amnesic effect of scopolamine: 100% of animals that had reached the learning criterion, and the antiamnestic activity was 106.4%.

Thus, the synthesized compounds demonstrate pronounced nootropic properties by modulating neurotransmitter systems, particularly the cholinergic system, which, in turn, can stimulate neurogenesis and promote the restoration of neuroplasticity. These properties indicate the possibility of using these substances as effective pharmacological tools for the prevention and correction of cognitive dysfunctions and neurological disorders resulting from COVID-19 transmission, and for improving memory in traumatic brain injuries and neurodegenerative diseases.

Acknowledgement

The authors gratefully acknowledge the financial support from the National University of Pharmacy.

Funding

The S.M.K. acknowledges Grant № 87/0062 (2021.01/0062) “Molecular design, synthesis and screening of new potential antiviral pharmaceutical ingredients for the treatment of infectious diseases COVID-19” from the National Research Foundation of Ukraine.

Availability of data and materials

The data generated in this study are presented in the figures and tables of this article. The other data generated in the present study may be requested from the corresponding author.

Ethics approval and consent to participate

We confirm that this study was conducted in full compliance with ethical standards. All laboratory animal procedures were approved by the Bioethics Committee of the National University of Pharmacy, Ukraine (Approval No. 12/2024, protocol 10.01.2024). Experiments complied with the European Convention for the Protection of Vertebrate Animals (1986, revised 1998), Directive 2010/63/EU, and Ukrainian legislation (Law No. 3446-IV, 2006).

AI use disclosure

Not applicable.

Conflict of interest

The authors declare no conflict of interest.

References

1. Sharif Sharif S, Guirguis A, Fergus S, Schifano F. The use and impact of cognitive enhancers among university students: a systematic review. Brain Sci. 2021;11(3):355.
2. Hou Y, Dan X, Babbar M, Wei Y, Hasselbalch SG, Croteau DL, et al. Ageing as a risk factor for neurodegenerative disease. Nat Rev Neurol. 2019;15(10):565-581.
3. Kovacs GG. Concepts and classification of neurodegenerative diseases. Handb Clin Neurol. 2017;145:301-307.
4. Jones C, Harasym J, Miguel-Cruz A, Chisholm S, Smith-MacDonald L, Brémault-Phillips S. Neurocognitive assessment tools for military personnel with mild traumatic brain injury: scoping literature review. JMIR Ment Health. 2021;8(2):e26360.
5. Moore BA, Brock MS, Brager A, Collen J, LoPresti M, Mysliwiec V. Posttraumatic stress disorder, traumatic brain injury, sleep, and performance in military personnel. Sleep Med Clin. 2020;15(1):87-100.
6. Adamescu AI, Tilișcan C, Stratan LM, Mihai N, Ganea OA, Miron VD, et al. The role of IL-6 and IL-1 in COVID-19 disease progression: the impact of gender-based differences, BMI variability and co-medications. Farmacia. 2025;73(2):308-316.
7. Wood GK, Sargent BF, Ahmad ZU, Tharmaratnam K, Dunai C, Egbe FN, et al. Posthospitalization COVID-19 cognitive deficits at 1 year are global and associated with elevated brain injury markers and gray matter volume reduction. Nat Med. 2025;31(1):245-257.
8. Nakamura T, Zou K, Shibuya Y, Michikawa M. Oral dysfunctions and cognitive impairment/dementia. J Neurosci Res. 2021;99(2):518-528.
9. Ball HA, McWhirter L, Ballard C, Bhome R, Blackburn DJ, Edwards MJ, et al. Functional cognitive disorder: dementia's blind spot. Brain. 2020;143(10):2895-2903.
10. Avan A, Hachinski V. Global, regional, and national trends of dementia incidence and risk factors, 1990-2019: a Global Burden of Disease study. Alzheimers Dement. 2023;19(4):1281-1291.
11. Wimo A. Long-term effects of Alzheimer's disease treatment. Lancet Neurol. 2015;14(12):1145-1146.
12. Breijyeh Z, Karaman R. Comprehensive review on Alzheimer's disease: causes and treatment. Molecules. 2020;25(24):5789.
13. Martino MV, Guandalini L, Di Cesare Mannelli L, Menicatti M, Bartolucci G, Dei S, et al. Piperazines as nootropic agents: new derivatives of the potent cognition-enhancer DM235 carrying hydrophilic substituents. Bioorg Med Chem. 2017;25(6):1795-1803.
14. Sendrowski K, Sobaniec W, Stasiak-Barmuta A, Sobaniec P, Popko J. Study of the protective effects of nootropic agents against neuronal damage induced by amyloid-beta (fragment 25-35) in cultured hippocampal neurons. Pharmacol Rep. 2015;67(2):326-331.
15. Thomas AB, Nanda RK, Kothapalli LP, Hamane SC. Synthesis and biological evaluation of Schiff's bases and 2-azetidinones of isonicotinyl hydrazone as potential antidepressant and nootropic agents. Arab J Chem. 2016;9(1):S79-S90.
16. Kang M, Lee DB, Kwon S, Lee E, Kim WJ. Effectiveness of nootropics in combination with cholinesterase inhibitors on cognitive function in mild-to-moderate dementia: a study using real-world data. J Clin Med. 2022;11(16):4661.
17. Patel CN, Georrge JJ, Modi KM, Narechania MB, Patel DP, Gonzalez FJ, et al. Pharmacophore-based virtual screening of catechol-o-methyltransferase (COMT) inhibitors to combat Alzheimer's disease. J Biomol Struct Dyn. 2018;36(15):3938-3957.
18. Javed MA, Ashraf N, Saeed Jan M, Mahnashi MH, Alqahtani YS, Alyami BA, et al. Structural modification, in vitro, in vivo, ex vivo, and in silico exploration of pyrimidine and pyrrolidine cores for targeting enzymes associated with neuroinflammation and cholinergic deficit in Alzheimer's disease. ACS Chem Neurosci. 2021;12(21):4123-4143.
19. Wilms W, Woźniak-Karczewska M, Corvini PFX, Chrzanowski Ł. Nootropic drugs: methylphenidate, modafinil and piracetam - population use trends, occurrence in the environment, ecotoxicity and removal methods - a review. Chemosphere. 2019;233:771-785.
20. Li Petri G, Raimondi MV, Spanò V, Holl R, Barraja P, Montalbano A. Pyrrolidine in drug discovery: a versatile scaffold for novel biologically active compounds. Top Curr Chem (Cham). 2021;379(5):34.

21. Pant S, Gupta M, Anthwal T, Chauhan M, Nain S. Neuroprotective effects of novel pyrrolidine-2-one derivatives on scopolamine-induced cognitive impairment in mice: behavioral and biochemical analysis. Pharmacol Biochem Behav. 2023;229:173602.
22. Gupta M, Kumar A, Prasun C, Nair MS, Kini SG, Yadav D, et al. Design, synthesis, extra-precision docking, and molecular dynamics simulation studies of pyrrolidin-2-one derivatives as potential acetylcholinesterase inhibitors. J Biomol Struct Dyn. 2023;41(13):6282-6294.
23. Malík M, Tlustoš P. Nootropics as cognitive enhancers: types, dosage and side effects of smart drugs. Nutrients. 2022;14(16):3367.
24. Cummings JL, Tong G, Ballard C. Treatment combinations for Alzheimer's disease: current and future pharmacotherapy options. J Alzheimers Dis. 2019;67(3):779-794.
25. Sharma K. Cholinesterase inhibitors as Alzheimer's therapeutics (review). Mol Med Rep. 2019;20(2):1479-1487.
26. Fayez AM, Elnoby AS, Bahnasawy NH, Hassan O. Neuroprotective effects of zafirlukast, piracetam and their combination on L-methionine-induced vascular dementia in rats. Fundam Clin Pharmacol. 2019;33(6):634-648.
27. Paliwal P, Dash D, Krishnamurthy S. Pharmacokinetic study of piracetam in focal cerebral ischemic rats. Eur J Drug Metab Pharmacokinet. 2018;43(2):205-213.
28. Niu F, Sharma A, Wang Z, Feng L, Muresanu DF, Sahib S, et al. Nanodelivery of oxiracetam enhances memory, functional recovery and induces neuroprotection following concussive head injury. Prog Brain Res. 2021;265:139-230.
29. Atwood R, Walker P, Walper D, Elster E, Bradley M. Use of levetiracetam for post-traumatic seizure prophylaxis in combat-related traumatic brain injury. Mil Med. 2023;188(11-12):e3570-e3574.
30. Wang L, Guo H, Zhao W, Wang J, Cao X. Oxiracetam ameliorates neurological function after traumatic brain injury through competing endogenous RNA regulatory network. Psychopharmacology (Berl). 2025;242(7):1231-1245.
31. Navarro SA, Serafim KGG, Mizokami SS, Hohmann MSN, Casagrande R, Verri WA. Analgesic activity of piracetam: effect on cytokine production and oxidative stress. Pharmacol Biochem Behav. 2013;105:183-192.
32. Schifano F, Bonaccorso S, Arillotta D, Corkery JM, Floresta G, Papanti Pelletier GD, et al. Focus on cognitive enhancement: a narrative overview of nootropics and "smart drug" use and misuse. Biology (Basel). 2025;14(9):1244.
33. Semenets AP, Suleiman MM, Fedosov AI, Shtrygol SY, Havrylov IO, Mishchenko MV, et al. Synthesis, docking, and biological evaluation of novel 1-benzyl-4-(4-(R)-5-sulfonylidene-4,5-dihydro-1H-1,2,4-triazol-3-yl)pyrrolidin-2-ones as potential nootropic agents. Eur J Med Chem. 2022;244:114823.
34. Morris GM, Huey R, Lindstrom W, Sanner MF, Belew RK, Goodsell DS, et al. AutoDock4 and AutoDockTools4: Automated docking with selective receptor flexibility. J Comput Chem. 2009;30(16):2785-91.
35. Ahmed AH, Oswald RE. Piracetam defines a new binding site for allosteric modulators of alpha-amino-3-hydroxy-5-methyl-4-isoxazole-propionic acid (AMPA) receptors. J Med Chem. 2010;53(5):2197-2203.
36. Brown AJH, Bradley SJ, Marshall FH, Brown GA, Bennett KA, Brown J, et al. From structure to clinic: Design of a muscarinic M1 receptor agonist with potential to treatment of Alzheimer's disease. Cell. 2021;184(24):5886-5901.e22.
37. Perekhoda L, Suleiman M, Podolsky I, Semenets A, Kobzar N, Yaremenko V, et al. Synthesis and nootropic activity prediction of some 4-(aminomethyl)-1-benzylpyrrolidin-2-one derivatives structurally related with nebracetam. ScienceRise Pharm Sci. 2024;4(50):23-34.
38. Podolsky I, Shtrygol' S. The memory and learning enhancing effects of atristamine. Pharmacia. 2019;66(1):13-18.
39. Havrylov I, Shtrygol' S. Investigation of the effect of a modified fragment of neuropeptide Y on memory phases and extrapolation escape task of animals. Ceska Slov Farm. 2021;70(3):91-99.
40. Festing MF, Altman DG. Guidelines for the design and statistical analysis of experiments using laboratory animals. ILAR J. 2002;43(4):244-258.
41. European Parliament and Council. Directive 2010/63/EU of the European Parliament and of the Council of 22 September 2010 on the protection of animals used for scientific purposes. Off J Eur Union. 2010;L276:33-79.
42. Vialko A, Chałupnik P, Szymańska E. Positive AMPA and kainate receptor modulators and their therapeutic potential in CNS diseases: a comprehensive review. Int J Mol Sci. 2025;26(13):6450.
43. Thal DM, Sun B, Feng D, Nawaratne V, Leach K, Felder CC, et al. Crystal structures of the M1 and M4 muscarinic acetylcholine receptors. Nature. 2016;531(7594):335-340.
44. Kruse AC, Kobilka BK, Gautam D, Sexton PM, Christopoulos A, Wess J. Muscarinic acetylcholine receptors: novel opportunities for drug development. Nat Rev Drug Discov. 2014;13(7):549-560.
45. Satoh R, Kawakami K, Nakadate K. Effects of smart drugs on cholinergic system and non-neuronal acetylcholine in the mouse hippocampus: histopathological approach. J Clin Med. 2022;11(12):3310.